Cellular Physiology and Biochemistry

Cell Physiol Biochem 2018;50:783-797
DOI: 10.1159/000494243
Published online: 12 October 2018
Accepted: 3 October 2018

Original Paper

Gp91^{phox} (NOX_2) in Activated Microglia Exacerbates Neuronal Damage Induced by Oxygen Glucose Deprivation and Hyperglycemia in an in Vitro Model

Xianzhang Zeng Hongliang Ren Yana Zhu Ruru Zhang Xinxin Xue Tao Tao Hongjie Xi

Department of Anaesthesiology, Second Affiliated Hospital of Harbin Medical University, Heilongjiang, China

Key Words
Hyperglycemia • Oxygen glucose deprivation • Gp91^{phox}siRNA

Abstract
Background/Aims: Peri-operative cerebral ischemia reperfusion injury is one of the most serious peri-operative complications that can be aggravated in patients with diabetes. A previous study showed that microglia NOX_2 (a NADPH oxidase enzyme) may play an important role in this process. Here, we investigated whether increased microglial derived gp91^{phox}, also known as NOX2, reduced oxygen glucose deprivation (OGD) after induction of hyperglycemia (HG). ***Methods:*** A rat neuronal-microglial *in vitro* co-culture model was used to determine the effects of gp91^{phox} knockdown on OGD after HG using six treatment groups: A rat microglia and neuron co-culture model was established and divided into the following six groups: high glucose + scrambled siRNA transfection (HG, n = 5); HG + gp91^{phox}siRNA transfection (HG-gp91siRNA, n = 5); oxygen glucose deprivation + scrambled siRNA transfection (OGD, n = 5); OGD + gp91^{phox}siRNA transfection (OGD-gp91siRNA, n = 5); HG + OGD + scrambled siRNA transfection (HG-OGD, n = 5); and HG + OGD + gp91^{phox}siRNA transfection (HG-OGD-gp91siRNA, n = 5). The neuronal survival rate was measured by the MTT assay, while western blotting was used to determine gp91^{phox} expression. Microglial derived ROS and neuronal apoptosis rates were analyzed by flow cytometry. Finally, the secretion of cytokines, including IL-6, IL-8, TNF-α, and 8-iso-PGF2α was determined using an ELISA kit. ***Results:*** Neuronal survival rates were significantly decreased by HG and OGD, while knockdown of gp91^{phox} reversed these rates. ROS production and cytokine secretion were also significantly increased by HG and OGD but were significantly inhibited by knockdown of gp91^{phox}siRNA. ***Conclusion:*** Knockdown of gp91^{phox}siRNA significantly reduced oxidative stress and the inflammatory response, and alleviated neuronal damage after HG and OGD treatment in a rat neuronal-microglial co-culture model.

X. Zeng and H. Ren contributed equally to this work.

Hongjie Xi
Department of Anaesthesiology, Second Affiliated Hospital of Harbin Med.Univ.
246 Xuefu Road, Harbin 150001, Heilongjiang (China)
Tel. 0086-0451-86605029, E-Mail xihongjie1973@163.com

Introduction

Cerebral ischemia reperfusion injury (CIRI), which is one of the most serious peri-operative complications, leads to a lower quality of life and an increased mortality rate. An animal study demonstrated that aging is related to the increase in some endogenous protein, which may contribute to decreased brain ischemic tolerance [1]. Therefore, as the population ages, an increased incidence of peri-operative CIRIs is expected; at the same time, the incidence of diabetes has been increasing year-by-year. According to the 2015 World Diabetes Congress survey, nearly 415 million adults worldwide have diabetes. It has been confirmed that the incidence and extent of CIRI increase in diabetic patients [2]. Thus, it is of great importance to investigate the pathogenesis and treatment of CIRI in patients with diabetes.

Previous studies have confirmed that systemic inflammation affects central nervous system responses [3], and both oxidative stress and inflammatory responses play an important role in the development and progression of CIRI and diabetes mellitus [4, 5]. Oxidative stress is essential in the development of injury following CIRI [6] and these effects are known to be exacerbated in patients with diabetes [7]. Additionally, the inflammation induced by CIRI is significantly enhanced in patients with diabetes [8]. An *in vitro* study also found that high glucose induces ROS production and activates cytokine secretion [9]. The expression of calcium sensing receptor in hippocampal neurons also decreased after treatment with high glucose and then increases the production of ROS in mitochondria [10]. Recently, it has been suggested that microglial activation following ischemia likely contributes to neuronal damage via release of excessive inflammatory cytokines and reactive oxygen species (ROS) [11]. Other studies have demonstrated that NOX_2, a NADPH oxidase enzyme, plays an important role in the CIRI process. The absence of NOX_2 can markedly reduce the production of oxidative stress and inflammatory responses, which significantly decreases the edema, blood-brain barrier destruction, and extent of brain damage associated with CIRI [12]. Whether NOX_2 is a target of therapy when patients with diabetes undergo CIRI is still unknown.

Our previous study showed that inhibition of NOX_2 may lead to the subsequent inhibition of oxidative stress and inflammation after CIRI in diabetic rats, and that microglia were likely the primary source of increased NOX_2 [13]. In consideration of another study [14], the findings of which were consistent, in part, with our previous above findings, we initiated an *in vitro* study to simulate CIRI in diabetes to investigate whether increased expression of microglial derived $gp91^{phox}$, also termed NOX_2, reduces oxygen glucose deprivation (OGD) after induction of hyperglycemia (HG).

Materials and Methods

Cell culture: rat microglia cells and neurons

The rat microglia cell line was purchased from Bioleaf (Shanghai, China) and cultured in DMEM medium (Gibco, Gaithersburg, MD, USA), supplemented with 10% fetal calf serum, 100 U/mL of penicillin, and 100 mg/mL of streptomycin. Cells were cultured at 37 °C in an atmosphere of 5% CO_2 in 95% air in a humidified incubator.

Use of progeny was approved by the Animal Center of the Second Affiliated Hospital of Harbin Medical University. Primary hippocampal neuronal cells were isolated from day-old neonate SD rats and cultured as described previously [15, 16]. Briefly, animals were euthanized and brains were removed, placed in culture dishes, washed in sterile Hank's balanced salt solution (HBSS; Hyclone, Logan, UT, USA) after which the meninges was removed and the hippocampus was carefully dissected out. Hippocampal tissues were washed with sterile HBSS, cut into small pieces (approximately 2 × 2 mm^2) and digested with 0.05% trypsin for 20 min at 37 °C, and the digestion procedure was stopped by adding 5mL DMEM. The resultant cell suspension was then filtered through cell strainer (70 μm) and was centrifuged at 1000 × *g* at for 5 min room temperature. After removing supernatant and adding 3–5 mL of DMEM medium, cells were

resuspended to a density of 1×10^6/L. Neuronal suspension (1mL) were inoculated in six cell culture plate coated with L-poly lysine (Sigma, St. Louis, MO, USA) and were cultured in a humidified 5% CO_2 atmosphere at 37 °C. After 4–6 h, when the neurons were adherent, the medium was changed to neurobasal-A medium, consisted of 94% neurobasal-A, 2% glutamine, 2% B27, and 2% penicillin and streptomycin (Gibco). Two-thirds of the culture medium was replaced every 3 days.

Transfection of rat microglia cells with gp91^{phox}siRNA

For transfections, approximately 5×10^5 of microglial were seeded into six-well culture plates and incubated overnight. Transfection with gp91^{phox} siRNA oligo (Genma, Suzhou, China) was performed using Lipofectamine 2000 (Invitrogen, Carlsbad, CA, USA). Cells were incubated with 2 μL of 100 nmol/L siRNA and 6 μL of Lipofectamine in 1 mL of Opti-MEM medium (Gibco) according to the manufacturer's protocol. Transfected cells were incubated for 6 h after which Opti-MEM medium was replaced by standard culture medium. Twenty-four hours after transfection, a second transfection was performed, which lasted for 48 h.

Western blotting and real-time PCR analysis for the optimal gp91^{phox} siRNA

Three kinds of gp91phoxsiRNA (siRNA1, siRNA2, and siRNA3) were designed for screening the best gp91phoxsiRNA to inhibit the expression of gp91phox; the scrambled siRNA was used as a negative control. At 72 h post-transfection, cells were harvested and washed with phosphate-buffered saline (PBS) for subsequent protein expression analysis. Initially, protein samples from all experimental protocols were obtained by cell lysis in RIPA lysis buffer (Beyotime Biotechnology, Jiangsu, China) in the presence of the proteinase inhibitor, phenylmethanesulfonyl fluoride (PMSF; Sigma). After elimination of cell debris by centrifugation, protein samples were quantified and equal quantities were separated by 8% sodium dodecyl sulfate–polyacrylamide gel electrophoresis (SDS-PAGE). Resolved proteins were then transferred onto PVDF membranes (Millipore, Billerica, MA, USA), which were blocked with 5% non-fat milk for 2 h, incubated with primary antibodies against gp91^{phox} (1:1000; BD, New York, NY, USA) or GADPH (1:1000; ZSGB-Bio, Beijing, China) overnight at 4 °C followed by a goat anti-rabbit secondary antibody (ZSGB-Bio) coupled to horseradish peroxidase for 2 h at room temperature. Protein bands were then visualized using BeyoECL Plus (Beyotime Biotechnology) in the GelDoc-2000 imaging system, Bio-RAP. The relative expression of gp91^{phox} was normalized to internal GADPH.

For PCR analysis, cells were culture as above and were then transfected with gp91^{phox}siRNA or the scrambled siRNA for 72 h. Total RNA was isolated using a High-pure RNA Isolation kit (Roche, Basel, Switzerland). The concentration of total RNA was measured and reverse transcription was conducted using 10 μL of total RNA (25 nmol/L) with the Transcriptor First Strand cDNA Synthesis kit (Roche) according to the manufacturer's protocol. One microliter of cDNA was amplified in real-time PCR assays using SYBR Green Master (Roche) and the BIO-RAD System (Bio-Rad,Berkeley, CA, USA) according to the manufacturer's protocol. Cycling conditions of real-time PCR were set as follows: initial activation step, 3 min at 95 °C; and 40 cycles, 12 s at 95 °C and 40 s at 62 °C. GADPH was used as an internal control. The primer sequences used for qRT-PCR are listed as follows: Gp91^{phox}(NOX_2), 5-GAATCTCAGGCCAATCACTT-3 (Forward), 5-TGGTCTTGAACTCGTTATCCC-3 (Reverse); GADPH, 5-TCTCTGCTCCTCCCTGTTC-3 (Forward), and 5-ACACCGACCTTCACCATCT-3 (Reverse). According to results, we found the optimal gp91^{phox} siRNA inhibited the gp91^{phox} most effectively.

Neuronal MTT cytotoxicity assay to exclude the influence of hypertonic osmotic pressure

Cultured neurons were used for *in vitro* studies on day 7. Neuronal cells were seeded in six-well plates at an initial density of 10, 000 cells/well and were treated with 140 mmol/L glucose and 140 mmol/L mannitol for 48 h, after which 100 μL of 5 mg/mL of MTT in PBS was added to each well, and incubated for 4 h at 37 °C. To dissolve formazan crystals, 500 μL of dimethyl sulfoxide (DMSO; Sigma) was added. After shaking the six-well plate for 1 min, the absorbance was measured at 492 nm using a microplate reader (BioTek Epoch, Burlington, VT, USA). The 100% value, as the standard to assess cytotoxicity, was obtained from the optical density (OD) values assayed in untreated cells.

Establishment of a neuronal-microglial co-culture model

Rat microglia cells and hippocampal neuron were co-cultured using the Transwell system (Corning, Inc., Corning, NY, USA) as previously described, with several modifications [17]. Hippocampal neurons were cultured in the lower chamber while microglia was cultured in the upper chamber.

Experimental protocol and treatment

Cells were divided into the following six groups: high glucose stimulation + scrambled siRNA transfection (HG, n = 5); high glucose stimulation + gp91^{phox}siRNA transfection (HG-gp91siRNA, n = 5); oxygen glucose deprivation + scrambled siRNA transfection (OGD, n = 5); oxygen glucose deprivation + gp91^{phox}siRNA transfection (OGD-gp91siRNA, n = 5); high glucose stimulation + oxygen glucose deprivation + scrambled siRNA transfection (HG-OGD group, n = 5); and high glucose stimulation + oxygen glucose deprivation + gp91^{phox}siRNA transfection (HG-OGD-gp91siRNA, n = 5).

The treatments were performed 48 h after the microglia were transfected with gp91siRNA or scrambled siRNA. For the HG and HG-gp91siRNA groups, the co-cultured cells were incubated with 140 mmol/L of glucose for 48 h, then cultured in normal culture medium for 30 min. For the OGD and OGD-gp91siRNA groups, the co-cultured cells were incubated with normal glucose for 48 h, then were deprived of oxygen-glucose for 30 min. Finally, for the HG-OGD and HG-OGD-gp91siRNA groups, the co-cultured cells were first incubated with 140 mmol/L of glucose for 48 h, then deprived of oxygen-glucose for 30 min. Thereafter, all cells were washed twice with PBS and re-suspended for analysis. The experiment protocol is shown in Fig. 1.

Neuronal MTT cytotoxicity assay

The survival rate of hippocampal neurons was measured using the MTT assay. After treatment, 100 μL of 5 mg/mL of MTT in PBS was put into each well, and incubated for 4 h at 37 °C. To dissolve the formazan crystal, 500 μL of DMSO was added. After shaking six-well plate for 1 min, absorbance was measured at 492 nm by a microplate reader (BioTek Epoch). The 100% value as the standard to assess cytotoxicity was obtained from the OD values assayed in untreated cells.

Flow cytometry for detecting neurons apoptosis

The apoptosis rate of hippocampal neurons was detected using Annexin V FITC/PI apoptosis kit (4A Biotech, Beijing, China). After treatment, hippocampal neuron cells were digested by 2.5% trypsin and centrifugation at 1000 × *g* for 5 min and the supernatant was discarded. A pre-cooled buffer solution (PBS with calcium) was used for the preparation of a single cell suspension, then centrifuged at 1000 × *g* for 5 min, the supernatant was discarded, and binding buffer was added at a concentration of 1 × 10^6 cells/mL. Annexin V FITC (5 μL) was then added to the cell and gently mixed and incubated for 5 min at room temperature in the dark. After adding 10 μL of PI and 400 μL of PBS, the cells were immediately detected and analyzed using flow cytometry (BD FACSCalibur™ Flow Cytometry, BD Biosciences, Franklin Lakes, USA).

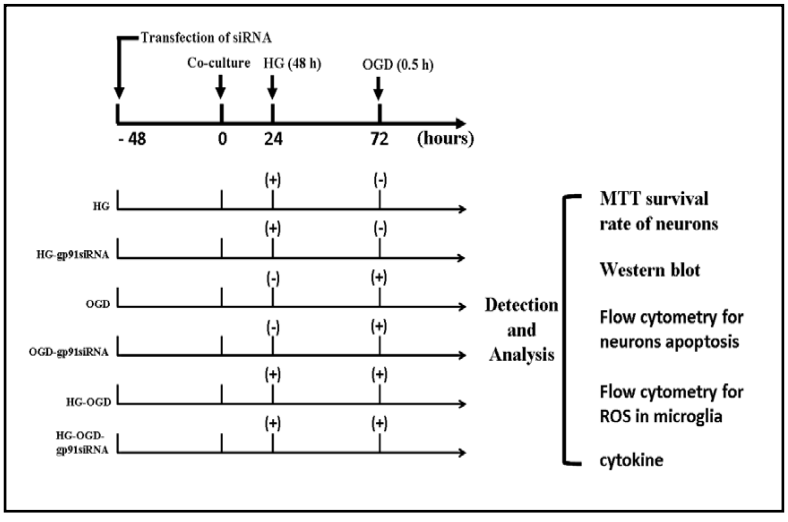

Fig. 1. Experimental protocol and experimental timeline for transfection, HG treatment, OGD, MTT survival rate of neurons, western blotting, flow cytometry, and culture medium cytokines.

A total of 1×10^4 cells were selected each time, and Cell Quest software was used to conduct data analysis. Annexin V-positive cells were apoptotic cells. Finally, the cell apoptosis rate of each group was calculated.

Western blotting analysis for gp91^{phox} expression

After treatment, cells were harvested and washed with PBS for subsequent analysis of gp91^{phox} protein expression by western blot as previously described in the *Western blotting and real-time PCR analysis for the optimal gp91^{phox} siRNA* section.

Measurement of intracellular ROS accumulation in microglial cells

Intracellular ROS accumulation was determined using a ROS assay kit (Jiancheng, Nanjing, China) that utilizes 2',7'-dichlorofluorescin diacetate (DCFH-DA) as a fluorescent probe. In principle, DCFH-DA freely penetrates the cell membrane and is hydrolyzed by esterase into DCFH, which is then oxidized by ROS resulting in a fluorescent green color. After high or normal glucose treatment, cells were incubated with 10 μmol of DCFH-DA for 45 min at 37 °C in the dark and washed twice with DMEM. For the HG-OGD, HG-OGD-gp91siRNA, OGD, and OGD-siRNA groups, the cells were deprived of oxygen-glucose for 30 min after incubation with DCFH-DA, washed twice with PBS and resulting fluorescent images were acquired using an inverted Olympus IX71 fluorescence microscope. The fluorescence intensities were measured by flow cytometry and reflected the amount of ROS that had been generated.

Enzyme-linked immunosorbent assay (ELISA) for cytokines

Cell culture supernatant levels of interleukin-6 (IL-6), interleukin-6 (IL-8), tumor necrosis factor-alpha (TNF-α), and 8-isoprostane were determined using commercial ELISA kits (Bio-Swamp, Shanghai, China). The culture supernatants of each group were not diluted prior to detection. Experimental procedures were performed according to the manufacturer's instructions. A microplate reader (BioTek Epoch, Winooski, VT, USA) was used to detect the OD values at 450 nm.

Statistical analysis

All statistical analyses were performed using SAS 9.3 international standard statistical programming software. Data are expressed as the mean ± standard deviation (SD). All experiments were assessed by a two-factor 2 × 3 factorial design ANOVA. A single effect comparison was performed when the interaction effect was found to be statistically significant. A $p < 0.05$ was considered significant for all statistical analyses.

Results

Neither gp91^{phox} siRNA nor hypertonic osmotic pressure result in neuronal damage

Fig. 2 A-C shows that transfection of the first gp91^{phox} siRNA resulted in maximum inhibition of gp91^{phox} expression ($p < 0.05$). Therefore, all subsequent experiments used the first gp91^{phox} siRNA. Fig. 2 D shows that only HG, but not the equal osmotic pressure of mannitol, resulted in significant neuronal damage ($p < 0.05$).

Transfection of microglia with gp91^{phox}siRNA significantly increases the survival rate of neurons

We used the MTT method to test the cytotoxicity of the neurons, with results showing that OGD combined with HG treatment significantly decreased the survival rate of neurons compared with either OGD or HG treatment alone (Fig. 3; $p < 0.0001$). Transfection of microglia with gp91^{phox}siRNA significantly increased the survival rate of neurons after either HG or OGD treatment alone and after a combination of HG and OGD treatment (Fig. 3; $p < 0.0001$).

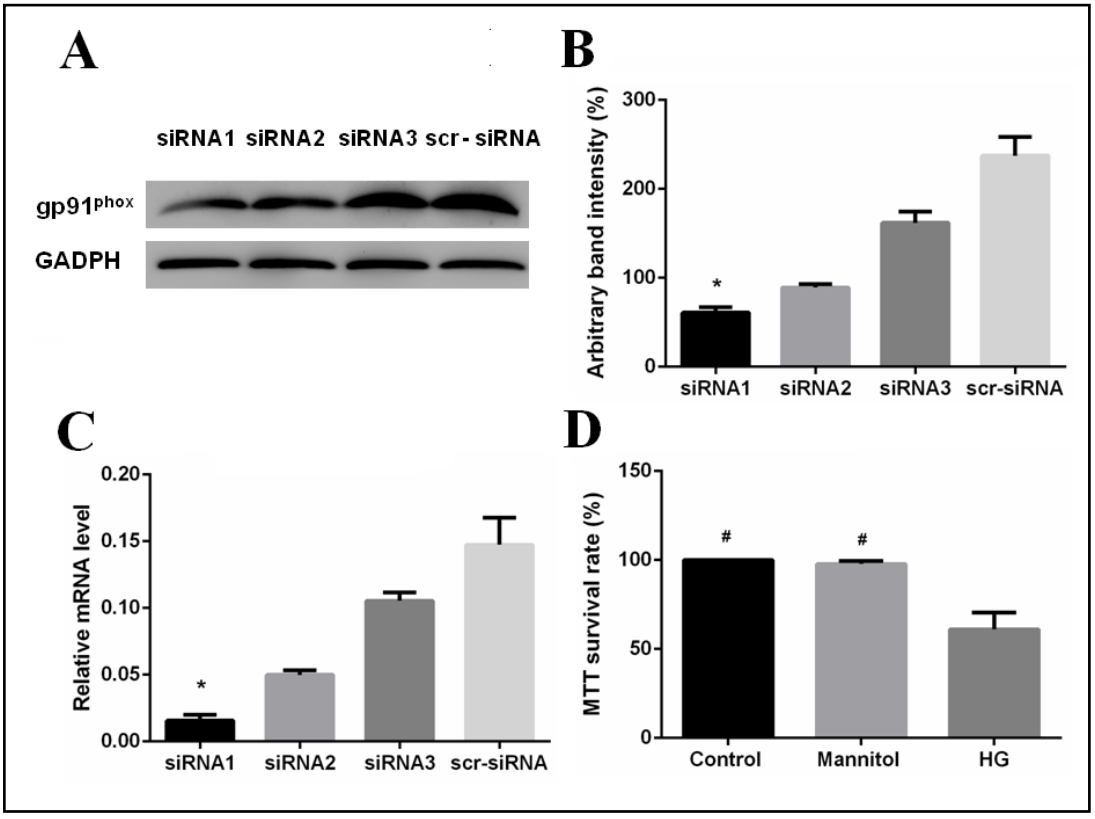

Fig. 2. Western blotting and real-time PCR analysis for the best gp91^{phox} siRNA and the cytotoxicity assay of the neurons by MTT to exclude the influence of hypertonic osmotic pressure. siRNA1, siRNA2, and siRNA3 were the three kinds of gp91^{phox}siRNA designed for screening out the best gp91^{phox}siRNA, which can inhibit the expression of gp91^{phox}. scr-siRNA was the scrambled siRNA used as the negative control. A, Representative western blot bands of gp91^{phox} (58 kDa) and GADPH (36 kDa) in the microglia 72 h after transfection. B, Quantification of western blot bands compared with GADPH (100%). C, Representative real-time PCR of gp91^{phox} and GADPH in the microglia 72 h after transfection. D, The cytotoxicity assay of the neurons by MTT to exclude the influence of hypertonic osmotic pressure after treatment with 140 mmol/L glucose and 140 mmol/L mannitol for 48 h. * p<0.001 vs NC group, # p<0.001 vs HG group.

Fig. 3. The cytotoxicity assay of the neurons by MTT. * p<0.0001 vs. HG group or OGD group, # p<0.0001 vs. the corresponding siRNA group.

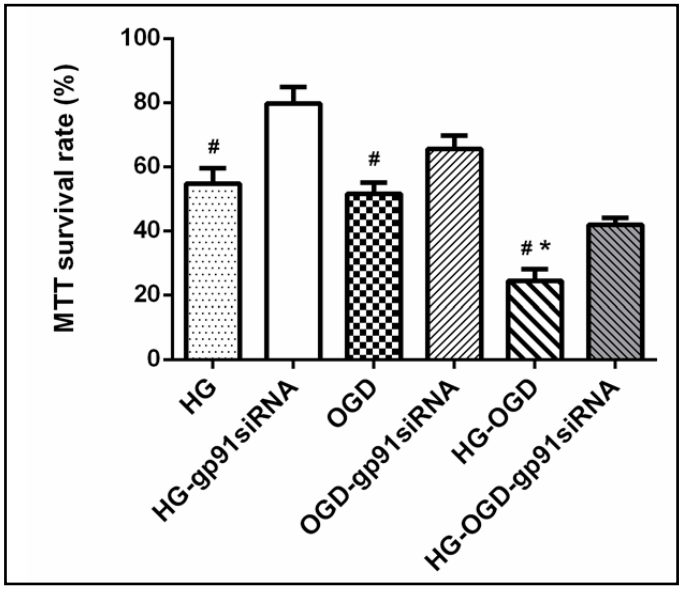

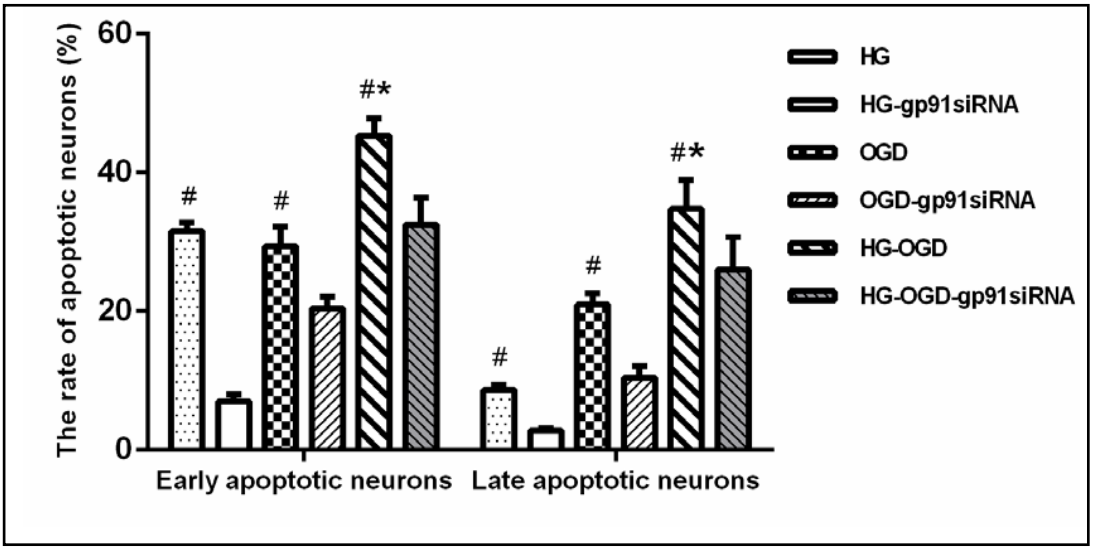

Fig. 4. Detection of neuron apoptosis. The percentages of viable, early and late apoptosis of neurons after HG, OGD, and HG combined with OGD treatment. * p<0.0001 vs. HG group or OGD group, # p<0.0001 vs. the corresponding siRNA group.

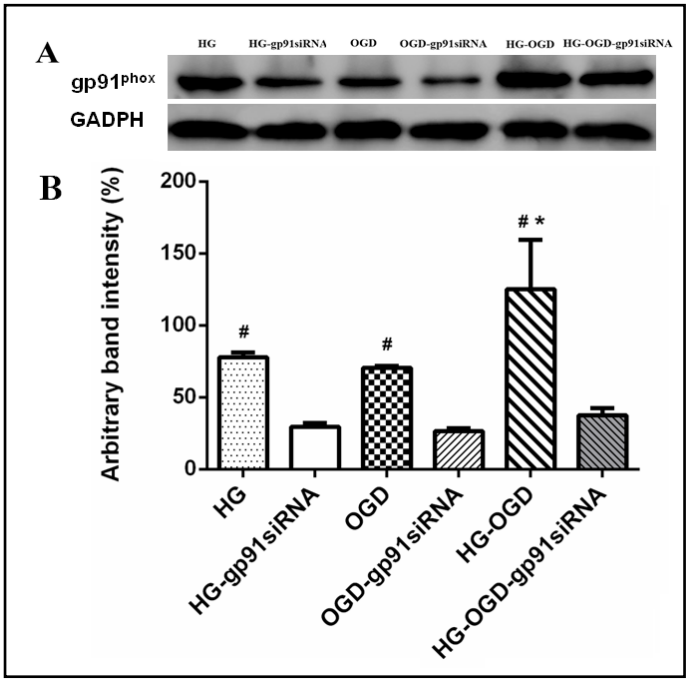

Fig. 5. Western blotting analysis for microglia gp91^{phox} protein. A, Representative western blot bands of gp91^{phox} (58 kDa) and GADPH (36 kDa) in the microglia 72 h after transfection in each group. B, Quantification of western blot bands compared with GADPH (100%). * p<0.0001 vs. HG group or OGD group, # p<0.0001 vs. the corresponding siRNA group.

Transfection of microglia with gp91^{phox}siRNA significantly decreases the neuronal apoptosis rate

Flow cytometry detection of FITC-Annexin V/PI double staining showed that OGD combined with HG treatment significantly increased the rate of apoptosis in neurons compared with OGD or HG treatment alone (Fig. 4; $p < 0.0001$). Transfection of microglia with gp91^{phox}siRNA significantly decreased the rate of apoptosis rate in neurons compared with the corresponding scrambled siRNA transfection groups (Fig. 4; $p < 0.0001$).

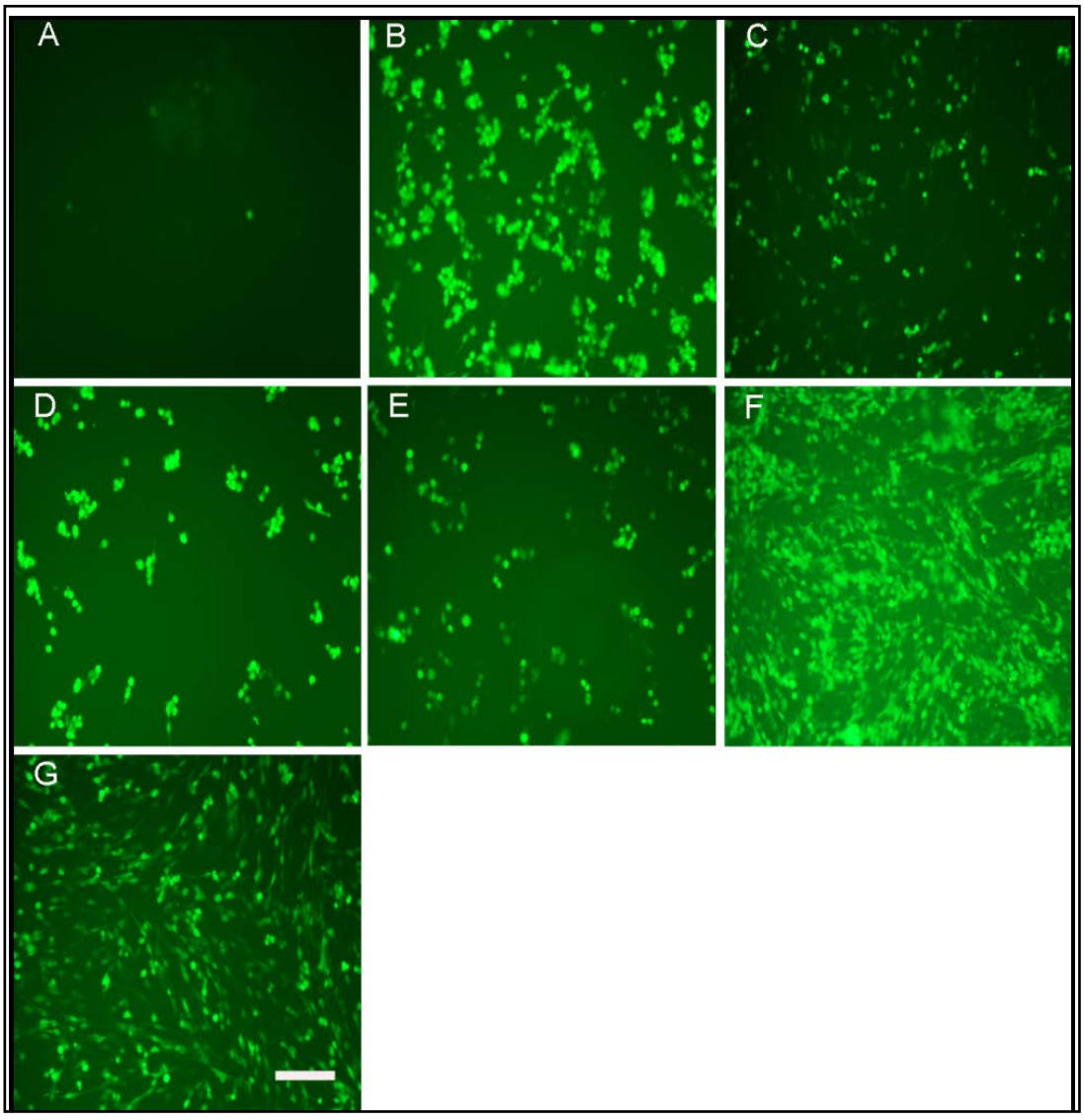

Fig. 6. The fluorescence images acquired by an inverted fluorescence microscope. The Microglia show green fluorescence. The ruler is 50 microns. A, Negative control. B, HG group. C, HG-gp91^{phox}siRNA group. D, OGD group. E, OGD- gp91^{phox}siRNA group. F, HG-OGD group. G, HG-OGD-gp91^{phox}siRNA group. Scale bars in G: 50 μm.

Transfection of microglia with gp91^{phox}siRNA significantly decreases the expression of gp91^{phox}

Immunoblotting experiments were used to determine the expression of gp91^{phox} after HG and OGD. Protein levels of gp91^{phox} were significantly increased after HG combined with OGD treatment compared with either OGD or HG treatment alone (Fig. 5; $p < 0.0001$). Transfection of microglia with gp91^{phox}siRNA significantly decreased gp91^{phox} expression after either HG treatment alone or OGD treatment alone, and after HG combined with OGD treatment (Fig. 5; $p < 0.0001$).

Inhibition of microglial gp91^{phox} expression reduces the production of ROS

Fluorescence images acquired by an inverted fluorescence microscope are shown in Fig. 6. with microglia shown in green. Flow cytometry was used to detect neuronal apoptosis with DCFH-DA staining (Fig. 7A). The fluorescence intensity reflected the amount of ROS generated after treatment is shown in Fig. 7B. Specifically, treatment of OGD after HG significantly promoted the production of ROS compared with OGD or HG alone ($p < 0.0001$). Inhibition of microglial gp91^{phox} significantly reduced the production of ROS ($p < 0.0001$).

Inhibition of microglial derived gp91^{phox} reduces the secretion of cytokines

The concentrations of IL-6 (Fig. 8A), IL-8 (Fig. 8B), TNF-α (Fig. 8C), and 8-iso-PGF2α (Fig. 8D) were determined using ELISA. In the HG-OGD group, the secretion of IL-6 was significantly increased compared with the HG and OGD treatment groups ($p < 0.0001$), as was secretion of IL-8 (HG treatment; $p < 0.05$ and OGD treatment; $p < 0.05$); however, there were no significant differences for either TNF-α or 8-iso-PGF2α. Inhibition of microglial gp91^{phox} expression reduced the secretion of all cytokines compared with the corresponding scrambled siRNA transfection groups ($p < 0.001$).

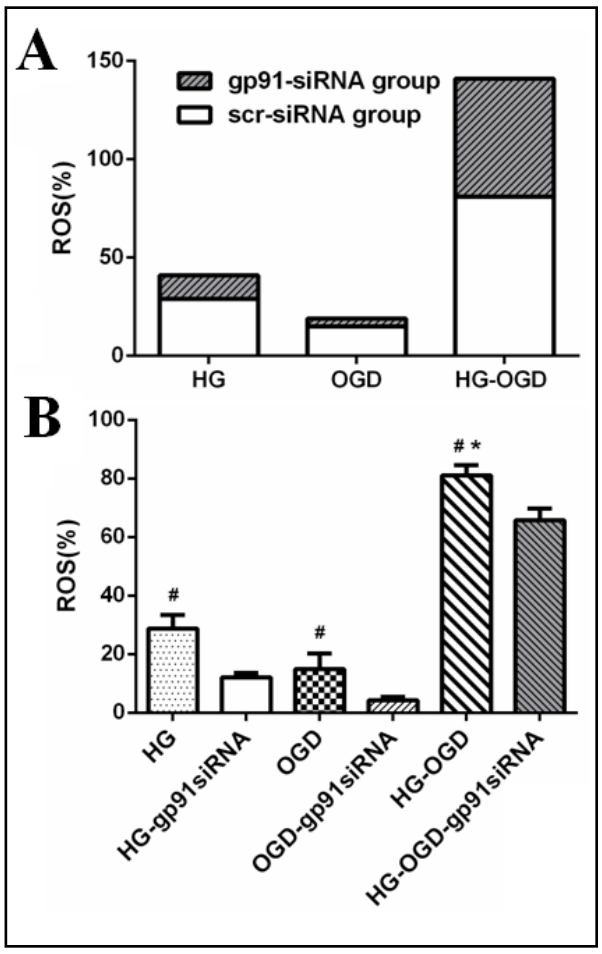

Fig. 7. Flow cytometry measurement of intracellular ROS accumulation in microglia. A, Comparison of the generated ROS between gp91siRNA and scrambled siRNA after HG, OGD, and HG combined with OGD treatment. B, The fluorescence intensity reflected the amount of ROS generated after HG, OGD, and HG combined with OGD treatment. * $p<0.0001$ vs. HG group or OGD group, # $p<0.0001$ vs. the corresponding siRNA group.

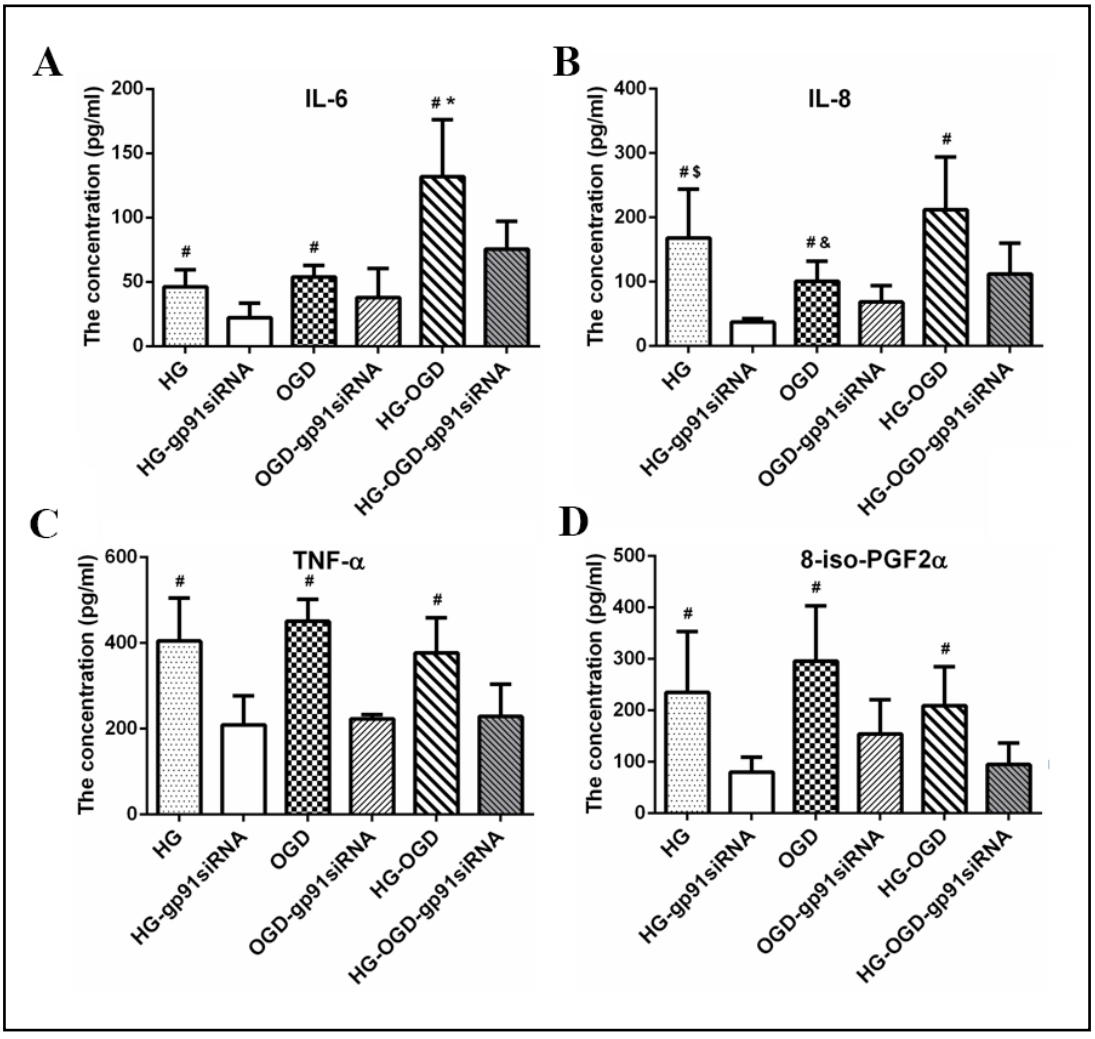

Fig. 8. IL-6, IL-8, TNF-α, 8-iso-PGF2α culture medium concentrations in each group. A, The concentration of IL-6. B, The concentration of IL-8. B, The concentration of TNF-α. D, The concentration of 8-iso-PGF2α. * p<0.0001 vs HG group or OGD group, # p<0.001 vs. the corresponding siRNA group, $ p<0.05 vs. HG-OGD group, & p<0.01 vs. HG-OGD group.

Discussion

In this *in vitro* study, we showed that both HG and OGD treatment increased neuronal apoptosis, and that apoptosis was further increased after treatment with a combination of these factors. Moreover, we also found that microglial derived $gp91^{phox}$ was significantly upregulated after both HG and OGD treatment and likely participated in neuronal apoptosis; furthermore, apoptotic mechanisms resulting from increased $gp91^{phox}$ expression were related to excessive inflammation and over-production of ROS. We believe this is the first *in vitro* neuronal-microglial co-culture study to elucidate the mechanism underlying the neuronal damage following HG and OGD exposure.

In a previous study, we investigated the protective effect of dexmedetomidine on transient global CIRI in diabetic rats [13]. The results showed that NOX_2 levels were significantly increased in diabetic rats compared with normal rats and were further increased when the diabetic rats were treated with transient global CIRI. Inhibition of NOX_2 in normal and diabetic rats subjected to CIRI was accompanied by decreased inflammation and oxidative

stress. Western blot analysis of Iba1 (Cyto) expression indicated that activated microglia were likely the main source of increased NOX_2. Therefore, we speculated that increased expression of NOX_2 derived from activated microglia may be a key therapeutic target for CIRI in patients with diabetes.

A previous study demonstrated that $gp91^{phox}$ immunoreactivity was dramatically increased in the peri-contusion region 2 days after traumatic brain injury. Although $gp91^{phox}$ is mainly expressed in activated microglia in the peri-contusion regions after traumatic brain injury, immunoreactive staining for $gp91^{phox}$ was also localized in astrocytes [14]. Another study indicated that stroke can result in an increase in T lymphocyte-derived NOX_2 dependent superoxide production in male mice, which and thus represents a major source of superoxide in the acute ischemia and reperfusion [18]. Thus, astrocytes and circulating T lymphocytes may influence the effects of microglia on neurons. The *in vitro* neuronal-microglial co-culture model in the current study excluded the influence of other cells, such as astrocytes and of hormones and immune cells of the circulatory system. We therefore conclude that HG and OGD treatment directly affected the expression of $gp91^{phox}$ by microglia, which in turn increased neuronal apoptosis through increased ROS and inflammation.

Microglia, which are the resident innate immune cells of the brain, are a chronic source of inflammation and ROS during progressive neuronal damage. Normally, microglia perform important functions, including the cleaning of cellular debris [19], neuronal support [20], and are also involved in innate immune defense [21]. Loss of normal microglial function is therefore deleterious [22]. Microglial derived NOX_2, which has been implicated as a prominent source of microglial ROS in pathology, is a key factor regulating microglial-mediated neurotoxicity, with many factors, such as cytokines, reported to initiate microglia NOX_2 expression [23]. Activated microglia produce extracellular ROS, which directly damages neurons [24-26], initiates intracellular signaling, enhances the pro-inflammatory response, and propagates neurotoxicity [27, 28]. In the present study, we showed that $gp91^{phox}$ was increased by both HG and OGD treatment and which was further increased following treatment with a combination of both. The results of our study indicated that microglia derived $gp91^{phox}$ is likely to be a key therapeutic target of OGD with HG. Transfection of microglia with $gp91^{phox}$ siRNA resulted in significantly decreased ROS production and secretion of cytokines significantly, which in turn led to decreased neuronal apoptosis.

In addition to the neuroprotective effects of genetic deletion of NOX_2 following CIRI, which have been confirmed by several studies [29, 30], oxidative stress is also involved in the etiology of diabetes [5]. There are three distinct mechanisms that have been established to generate ROS in neurons and to contribute to cell death during anoxia and re-oxygenation. Among these mechanisms, the NADPH oxidases, including NOX_2, predominantly cause ROS generation [31]. In addition to NOX_2, mitochondria also produce ROS. A previous study showed that type I diabetes induced by streptozotocin (STZ) does not lead to brain mitochondrial dysfunction, indicating that oxidative stress in type I diabetes is not directly related to mitochondrial dysfunction, but more likely to extra-mitochondrial factors [32]. Evidence suggests that NOX_2 may be a potential therapeutic target for the treatment of diabetes because of the production of excessive cellular ROS in diabetes [33]. NOX_2 deficiency can reduce ROS production, which decreases β-cell destruction and preserves islet function in STZ-induced diabetes [34]. Therefore, we speculate that in addition to the effects of OGD, NOX_2 also plays an important role in HG-induced neuronal damage. To exclude the potential influence of hypertonic osmotic pressure on neuronal damage, we used mannitol with an equal osmotic pressure to high glucose, which was used in our study to induce HG. The results showed that only HG, but not the equal osmotic pressure of mannitol, resulted in neuronal damage, indicating that HG is the dominant factor involved in neuronal damage.

In addition to CIRI, diabetes and impairments in glucose metabolism and insulin resistance in the brain have been suggested as a likely etiology of Alzheimer's disease (AD) [35, 36]. In recent years, the relationship between insulin signaling and neurocognitive function has been investigated. Under normal conditions, neurons in the cortex and hippocampus produce insulin, which modulates glucose metabolism and cognitive function;

however, abnormal insulin resistance may lead to the increased production of ROS, which then impairs mitochondrial function, further inducing cognitive dysfunction in Alzheimer's disease [37]. It has been documented that impaired glucose metabolism or mitochondrial dysfunction is one of the major pathologic changes observed in various neurodegenerative diseases [38]. In addition, a recent study demonstrated that hippocampal insulin resistance, without a change in blood glucose, can result in reduced hippocampal mTOR signalling and altered expression of markers of neurogenesis and synaptic function. Induction of insulin resistance in cultured hippocampal neurons showed similar results [39]. After regulating insulin signaling in the hippocampus, the learning ability and memory of AD mice improved [40]. These studies indicated that both abnormal glucose metabolism and insulin resistance can influence neurofunction, even without high glucose. According to the results of our study and the above-mentioned previous studies, we speculate that the beneficial effects of transfection of gp91^{phox} siRNA to microglia on HG and OGD may also be applied to chronic degenerative diseases, such as Alzheimer's disease. Only high glucose without insulin was exposed to neurons for 48 h in our study. Therefore, according to a previous study in which an *in vitro* insulin resistance model was established [38], it appears that there should not be insulin resistance and the impact of insulin resistance on neuron survival may be minimal. We believe, however, that further investigation should be considered with respect to insulin resistance, and the effect of the transfection of gp91^{phox} siRNA to microglia should also be applied to *in vivo* animal models, such as stroke in diabetes, because of the difference between *in vitro* and *in vivo* models.

Here, the highest rates of neuronal apoptosis were found in the HG-OGD group and likely occurred for two reasons: 1) HG produced a significant amount of ROS and secretion of cytokines; and 2) OGD further induced ROS production and cytokine secretion. As mentioned in previous studies, both HG and OGD were shown to induce oxidative damage, inflammation, and altered expression of matrix metalloproteinases (MMPs). OGD can induce oxidative stress, inflammatory cytokine accumulation, and MMP dissipation via NF-κB and ERK1/2 pathways in primary rat astrocytes. HG can result in the over-production of ROS and a loss of MMP [41-43]. Indeed, the results of this study showed that gp91phox is the common denominator in both processes. Therefore, although we did not test the expression of MMPs, inhibition of microglial gp91phox significantly decreased ROS production and cytokine, which in turn decreased neuronal apoptosis in the HG-OGD group.

There are several limitations to the current study. We did not test for apoptotic-related proteins. However, previous studies confirmed that ROS can cause cytotoxicity through lipid peroxidation, oxidation of proteins, and DNA fragmentation [44, 45]. Other studies demonstrated that increased levels of pro-inflammatory cytokines, including TNF-α and IL-6, can be observed at early stages in transient global ischemia [46]. As TNF-α predominately mediates immune and inflammatory responses that lead to apoptosis [47], we speculate that the protection endowed by knockdown of gp91^{pho}x after HG and OGD treatment may have resulted in the decreased ROS production and cytokine secretion observed in the current study. Thus, further investigation regarding the underlying apoptotic mechanisms related to the knockdown of gp91^{phox} is needed. Another limitation in this study was that we did not have access to *gp91^{phox}* knockout mice and therefore utilized siRNA technology, which only partially inhibited gp91^{phox} expression and thus may mask the dominant role of gp91^{phox}.

Conclusion

Here we show that ROS production and cytokine secretion from activated microglia, which express gp91^{phox}, play an important role in neuronal damage after HG and OGD treatment and that gp91^{phox} may be a key therapeutic target in alleviating this damage. Transfection of microglia with gp91^{phox}siRNA significantly reduced oxidative stress and the inflammatory response in neurons, which subsequently alleviated neuronal apoptosis; this may provide a new therapeutic strategy for patients with diabetes undergoing surgery.

Acknowledgements

This work was supported by grants from the National Natural Science Foundation of China (No. 81701288), and Innovation Research Fund of the Second Affiliated Hospital of Harbin Medical University (No. CX2016-08).

Disclosure Statement

The authors declare that they have no competing interests.

References

1 Li J, Shan W, Zuo Z: Age-related upregulation of carboxyl terminal modulator protein contributes to the decreased brain ischemic tolerance in older rats. Mol Neurobiol 2018;55:6145-6154.
2 Wei N, Yu SP, Gu XH, Chen DD, Whalin MK, Xu GL, Liu XF, Wei L: The involvement of autophagy pathway in exaggerated ischemic brain damage in diabetic mice. CNS Neurosci Ther 2013;19:753-763.
3 Pimenta FS, Ton AMM, Guerra TO, Alves GG, Campagnaro BP: Unmasking the gut-brain axis: How the microbiota influences brain and behavior. J Food Microbiol 2018;2:23-34.
4 Rajput MS, Sarkar PD, Nirmal NP: Inhibition of DPP-4 activity and neuronal atrophy with genistein attenuates neurological deficits induced by transient global cerebral ischemia and reperfusion in streptozotocin-induced diabetic mice. Inflammation 2017;40:623-635.
5 Tsuruta R, Fujita M, Ono T, Koda Y, Koga Y, Yamamoto T, Nanba M, Shitara M, Kasaoka S, Maruyama I, Yuasa M, Maekawa T: Hyperglycemia enhances excessive superoxide anion radical generation, oxidative stress, early inflammation, and endothelial injury in forebrain ischemia/reperfusion rats. Brain Res 2010;1309:155-163.
6 Shi H, Liu KJ: Cerebral tissue oxygenation and oxidative brain injury during ischemia and reperfusion. Front Biosci 2007;12:1318-1328.
7 Rains JL, Jain SK: Oxidative stress, insulin signaling, and diabetes. Free Radic Biol Med 2011;50:567-575.
8 Muthaian R, Pakirisamy RM, Parasuraman S, Raveendran R: Hypertension influences the exponential progression of inflammation and oxidative stress in streptozotocin-induced diabetic kidney. J Pharmacol Pharmacother 2016;7:159-164.
9 Dai J, Zhang X, Li L, Chen H, Chai Y: Autophagy inhibition contributes to ROS-producing NLRP3-dependent inflammasome activation and cytokine secretion in high glucose-induced macrophages. Cell Physiol Biochem 2017;43:247-256.
10 Dong S, Li G, Zheng D, Wu J, Sun D, Yang F, Yu X, Li T, Sun A, Liu J, Zhong X, Xu C, Lu F, Zhang W: A novel role for the calcium sensing receptor in rat diabetic encephalopathy. Cell Physiol Biochem 2015;35:38-50.
11 Lalancette-Hebert M, Phaneuf D, Soucy G, Weng YC, Kriz J: Live imaging of Toll-like receptor 2 response in cerebral ischaemia reveals a role of olfactory bulb microglia as modulators of inflammation. Brain 2009;132:940-954.
12 Chen H, Kim GS, Okami N, Narasimhan P, Chan PH: NADPH oxidase is involved in post-ischemic brain inflammation. Neurobiol Dis 2011;42:341-348.
13 Zeng X, Wang H, Xing X, Wang Q, Li W: Dexmedetomidine protects against transient global cerebral ischemia/reperfusion induced oxidative stress and inflammation in diabetic rats. PLoS One 2016;11:e0151620.
14 Dohi K, Ohtaki H, Nakamachi T, Yofu S, Satoh K, Miyamoto K, Song D, Tsunawaki S, Shioda S, Aruga T: Gp91phox (NOX2) in classically activated microglia exacerbates traumatic brain injury. J Neuroinflammation 2010;7:41.
15 Kaech S, Banker G: Culturing hippocampal neurons. Nat Protoc 2006;1:2406-2415.
16 Brewer GJ, Torricelli JR: Isolation and culture of adult neurons and neurospheres. Nat Protoc 2007;2:1490-1498.

17 Yamashita A, Soga Y, Iwamoto Y, Yoshizawa S, Iwata H, Kokeguchi S, Takashiba S, Nishimura F: Macrophage-adipocyte interaction: marked interleukin-6 production by lipopolysaccharide. Obesity (Silver Spring) 2007;15:2549-2552.
18 Brait VH, Jackman KA, Walduck AK, Selemidis S, Diep H, Mast AE, Guida E, Broughton BR, Drummond GR, Sobey CG: Mechanisms contributing to cerebral infarct size after stroke: gender, reperfusion, T lymphocytes, and Nox2-derived superoxide. J Cereb Blood Flow Metab 2010;30:1306-1317.
19 Rivest S: The promise of anti-inflammatory therapies for CNS injuries and diseases. Expert Rev Neurother 2011;11:783-786.
20 Morgan SC, Taylor DL, Pocock JM: Microglia release activators of neuronal proliferation mediated by activation of mitogen-activated protein kinase, phosphatidylinositol-3-kinase/Akt and delta-Notch signalling cascades. J Neurochem 2004;90:89-101.
21 Loane DJ, Byrnes KR: Role of microglia in neurotrauma. Neurotherapeutics 2010;7:366-377.
22 Streit WJ, Xue QS: Life and death of microglia. J Neuroimmune Pharmacol 2009;4:371-379.
23 Mander PK, Jekabsone A, Brown GC: Microglia proliferation is regulated by hydrogen peroxide from NADPH oxidase. J Immunol 2006;176:1046-1052.
24 Sundar IK, Caito S, Yao H, Rahman I: Oxidative stress, thiol redox signaling methods in epigenetics. Methods Enzymol 2010;474:213-244.
25 Brown GC, Neher JJ: Inflammatory neurodegeneration and mechanisms of microglial killing of neurons. Mol Neurobiol 2010;41:242-247.
26 Wang X, Michaelis EK: Selective neuronal vulnerability to oxidative stress in the brain. Front Aging Neurosci 2010;2:12.
27 Wang T, Qin L, Liu B, Liu Y, Wilson B, Eling TE, Langenbach R, Taniura S, Hong JS: Role of reactive oxygen species in LPS-induced production of prostaglandin E2 in microglia. J Neurochem 2004;88:939-947.
28 Qin L, Liu Y, Wang T, Wei SJ, Block ML, Wilson B, Liu B, Hong JS: NADPH oxidase mediates lipopolysaccharide-induced neurotoxicity and proinflammatory gene expression in activated microglia. J Biol Chem 2004;279:1415-1421.
29 Kahles T, Luedike P, Endres M, Galla HJ, Steinmetz H, Busse R, Neumann-Haefelin T, Brandes RP: NADPH oxidase plays a central role in blood-brain barrier damage in experimental stroke. Stroke 2007;38:3000-3006.
30 Chen H, Song YS, Chan PH: Inhibition of NADPH oxidase is neuroprotective after ischemia-reperfusion. J Cereb Blood Flow Metab 2009;29:1262-1272.
31 Abramov AY, Scorziello A, Duchen MR: Three distinct mechanisms generate oxygen free radicals in neurons and contribute to cell death during anoxia and reoxygenation. J Neurosci 2007;27:1129-1138.
32 Moreira PI, Santos MS, Moreno AM, Proenca T, Seica R, Oliveira CR: Effect of streptozotocin-induced diabetes on rat brain mitochondria. J Neuroendocrinol 2004;16:32-38.
33 Kowluru A, Kowluru RA: Phagocyte-like NADPH oxidase [Nox2] in cellular dysfunction in models of glucolipotoxicity and diabetes. Biochem Pharmacol 2014;88:275-283.
34 Xiang FL, Lu X, Strutt B, Hill DJ, Feng Q: NOX2 deficiency protects against streptozotocin-induced beta-cell destruction and development of diabetes in mice. Diabetes 2010;59:2603-2611.
35 Bedse G, Di Domenico F, Serviddio G, Cassano T: Aberrant insulin signaling in Alzheimer's disease: current knowledge. Front Neurosci 2015;9:204.
36 Hao K, Di Narzo AF, Ho L, Luo W, Li S, Chen R, Li T, Dubner L, Pasinetti GM: Shared genetic etiology underlying Alzheimer's disease and type 2 diabetes. Mol Aspects Med 2015;43-44:66-76.
37 Abolhassani N, Leon J, Sheng Z, Oka S, Hamasaki H, Iwaki T, Nakabeppu Y: Molecular pathophysiology of impaired glucose metabolism, mitochondrial dysfunction, and oxidative DNA damage in Alzheimer's disease brain. Mech Ageing Dev 2017;161(Pt A):95-104.
38 Bhat AH, Dar KB, Anees S, Zargar MA, Masood A, Sofi MA, Ganie SA: Oxidative stress, mitochondrial dysfunction and neurodegenerative diseases; a mechanistic insight. Biomed Pharmacother 2015;74:101-110.
39 Schmitz L, Kuglin R, Bae-Gartz I, Janoschek R, Appel S, Mesaros A, Jakovcevski I, Vohlen C, Handwerk M, Ensenauer R, Dötsch J, Hucklenbruch-Rother E: Hippocampal insulin resistance links maternal obesity with impaired neuronal plasticity in adult offspring. Psychoneuroendocrinology 2018;89:46-52.
40 Han K, Jia N, Zhong Y, Shang X: S14G-humanin alleviates insulin resistance and increases autophagy in neurons of APP/PS1 transgenic mouse. J Cell Biochem 2018;119:3111-3117.

41 Xu WW, Guan MP, Zheng ZJ, Gao F, Zeng YM, Qin Y, Xue YM: Exendin-4 alleviates high glucose-induced rat mesangial cell dysfunction through the AMPK pathway. Cell Physiol Biochem 2014;33:423-432.
42 Liang W, Chen M, Zheng D, Li J, Song M, Zhang W, Feng J, Lan J: The ppening of ATP-sensitive K+ channels protects H9c2 cardiac cells against the high glucose-induced injury and inflammation by inhibiting the ROS-TLR4-Necroptosis pathway. Cell Physiol Biochem 2017;41:1020-1034.
43 Xia R, Ji C, Zhang L: Neuroprotective effects of pycnogenol against oxygen-glucose deprivation/ reoxygenation-induced injury in primary rat astrocytes via NF-κB and ERK1/2 MAPK pathways. Cell Physiol Biochem 2017;42:987-998.
44 Crack PJ, Taylor JM: Reactive oxygen species and the modulation of stroke. Free Radic Biol Med 2005;38:1433-1444.
45 Gursoy-Ozdemir Y, Can A, Dalkara T: Reperfusion-induced oxidative/nitrative injury to neurovascular unit after focal cerebral ischemia. Stroke 2004; 35:1449-1453.
46 Zhu Y, Saito K, Murakami Y, Asano M, Iwakura Y, Seishima M: Early increase in mRNA levels of pro-inflammatory cytokines and their interactions in the mouse hippocampus after transient global ischemia. Neurosci Lett 2006;393:122-126.
47 Figiel I, Dzwonek K: TNFalpha and TNF receptor 1 expression in the mixed neuronal-glial cultures of hippocampal dentate gyrus exposed to glutamate or trimethyltin. Brain Res 2007;1131:17-28.